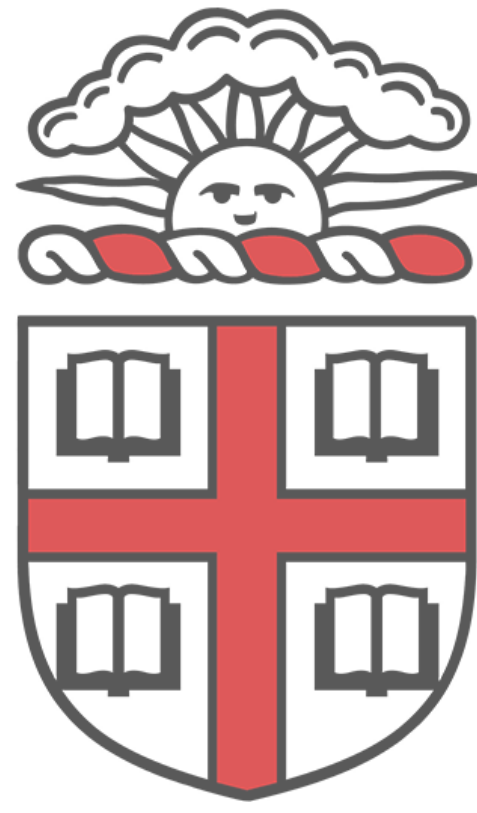


Radio Cosmology Lab | Exploring the Epoch of Reionization

Joshua Kerrigan, Adam Lanman, Wenyang Li, Jonathan Pober

Brown University Physics

21 cm @ COSMOLOGY



Introduction

Following the recombination of hydrogen and release of the cosmic microwave background radiation at redshift $z \sim 1100$, the baryonic matter of the universe consisted mostly of neutral hydrogen and helium. Gradually, small inhomogeneities collapsed and ignited the first luminous structures. Energetic photons emitted from the first stars and quasars reionized the surrounding medium, producing ionized bubbles which grew and merged into the fully ionized intergalactic medium we see today. This *Epoch of Reionization* (EoR) remains a poorly-understood period of the universe's history which offers a wealth of cosmological and astrophysical information.

The Pober lab is part of an international effort to build instruments capable of studying the EoR. The neutral hydrogen (HI) of the EoR emits faintly at a wavelength of 21cm, due to the hyperfine transition. This emission is unique to neutral hydrogen, and is anti-correlated with the ionized (HII) regions that fill the universe through the EoR. CMB constraints and quasar absorption spectra put the EoR as occurring within the redshift range $6 < z < 12$, which means 21cm emissions will redshift to meter scale wavelengths. This is accessible to modern radio interferometers, including the *Donald C. Backer Precision Array for Probing the Epoch of Reionization* (PAPER), the *Murchison Widefield Array* (MWA), and the recently-funded *Hydrogen Epoch of Reionization Array* (HERA).

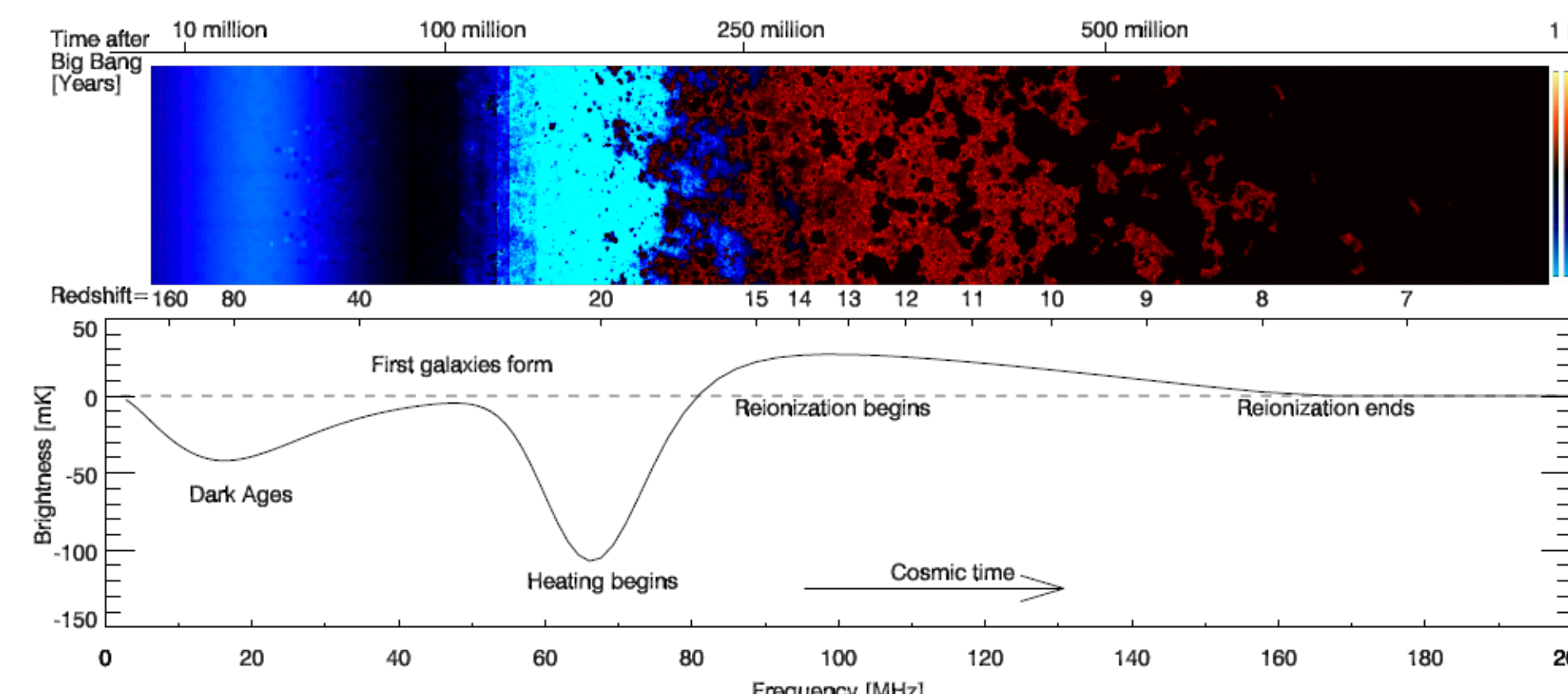


Figure 1: The global differential brightness temperature, δT_b , evolution over redshift $6 < z < 160$. δT_b becomes observable when the spin temperature T_S decouples from the CMB temperature, T_{CMB} through the Wouthuysen-Field effect, this can be seen in Eqn. 1

Differential Brightness Temperature

$$\delta T_b = 28 \text{ mK} (1 + \delta) x_{HI} \left(1 - \frac{T_{CMB}}{T_{spin}} \right) \left(\frac{\Omega_b h^2}{0.0223} \right) \sqrt{\left(\frac{1+z}{10} \right) \left(\frac{0.24}{\Omega_m} \right) \left[\frac{H(z)/(1+z)}{dv_{||}/d\tau_{||}} \right]} \quad (1)$$

The differential brightness temperature describes the complex nature of the neutral hydrogen spin temperature, T_S decoupling from the CMB background temperature T_{CMB} , the neutral fraction of Hydrogen, x_{HI} , and the mass density contrast, δ . δT_b also describes an important relationship between cosmological and astrophysical parameters, showing that measuring what is seen as a cosmological epoch has astrophysical relevance.

The Foreground Problem

Galactic and extragalactic foregrounds pose a difficult problem when trying to measure the 21cm EoR signal. Relative to galactic foregrounds, the EoR signal is ~ 5 orders of magnitude smaller than the galactic emissions that exist between our observing radio telescope arrays and the highly redshifted 21cm signal. The overlapping sources of power in our observations can be seen in Fig. 2.

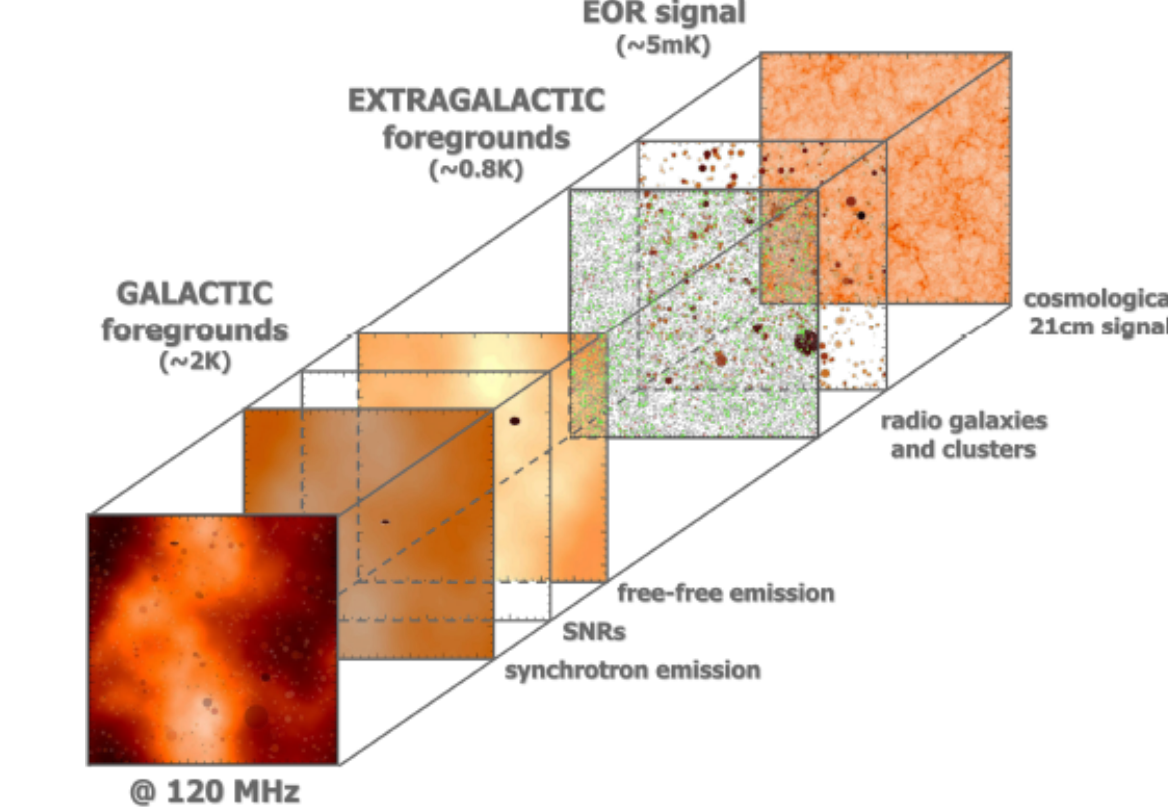


Figure 2: The various cosmological and galactic sources that contribute to the measured sky temperature, and their relative strengths. Source: Saleem Zaroubi, <https://ned.ipac.caltech.edu/level5/March14/Zaroubi/Zaroubi5.html>

To overcome foreground dominance in our power spectrum analysis we can use a combination of foreground power mitigating techniques as outlined in the following subsections.

Foreground Subtraction

Foreground subtraction is performed in the image domain using an extragalactic source catalog. The source catalog is used to generate a foreground model which can then be fit by an n^{th} order polynomial and subtracted from the observation.

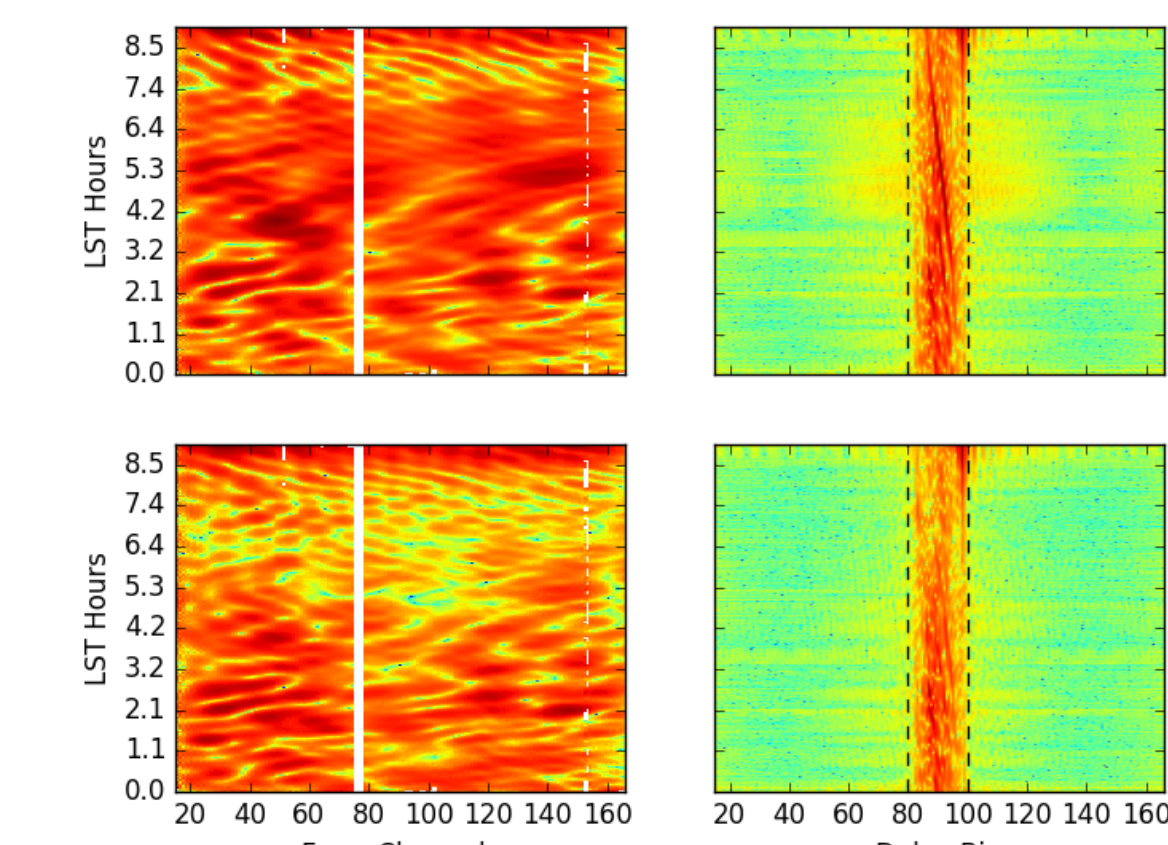


Figure 3: LST binned visibility of a 30m East-West baseline from the PAPER-64 array. The left plots show a baseline visibility pre- and post subtraction. The right plots show the delay transform of the left plots, demonstrating the foreground power being concentrated within the horizon limit (dotted lines).

Foreground Avoidance

$$V_b(\tau) = \int d\tau d\mu d\nu A(l, m, \nu) I(l, m, \nu) e^{-2\pi i \nu(\tau_g - \tau)} \quad (2)$$

Taking the Fourier transform of a baseline visibility over frequency with the geometric group delay offset (eqn. 2) results in smooth spectrum foregrounds bunching up nearest to the delay of $\tau = 0$. This is because foreground sources have a maximal geometric delay associated with a baseline length, $|b|$, which is also known as the horizon limit. The EoR signal is unsmooth spectrally, distinguishing it from foreground sources, and pushing it beyond the horizon limit imposed by the baseline length. Using this information, delays below the horizon limit can be filtered giving significant foreground power removal.

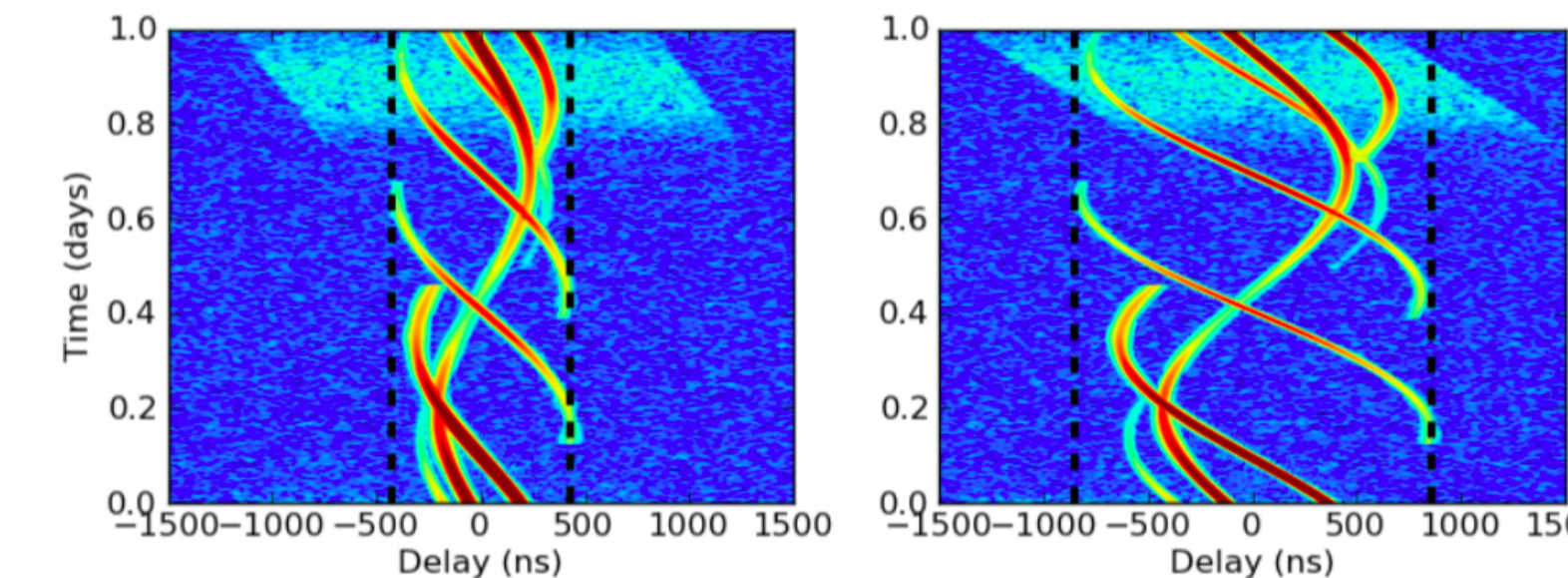


Figure 4: Delay transform visibilities of two different baseline types. Smooth spectral sources moving between delays over time can be seen to remain within the horizon limit (dotted), while unsmooth spectral sources (light blue) extend beyond the horizon limit. Source: Aaron Parsons, A Per Baseline Delay-Spectrum Technique for Accessing the 21cm Cosmic Reionization Signature, ApJ. 2012

Calibration

The most common techniques we use on visibility calibration are redundant calibration and sky model based calibration. Sky model calibration requires some preknowledges about the sky. With some assumptions about source structures about the sky and understanding of our instrument, we use FHD (Fast Holographic Deconvolution) to calibrate visibility data. The algorithm FHD uses is basically 'CLEAN' algorithm. Redundant calibration is sky model independent. All it assumes is that same antenna separations should measure exact the same Fourier mode of the sky. Redundant calibration requires antenna array with good redundant calibratability, like PAPER64 (The Precision Array for Probing the Epoch of Reionization), MWA (Murchison WideField Array) PhaseII hexes, HERA (Hydrogen Epoch of Reionization Array).

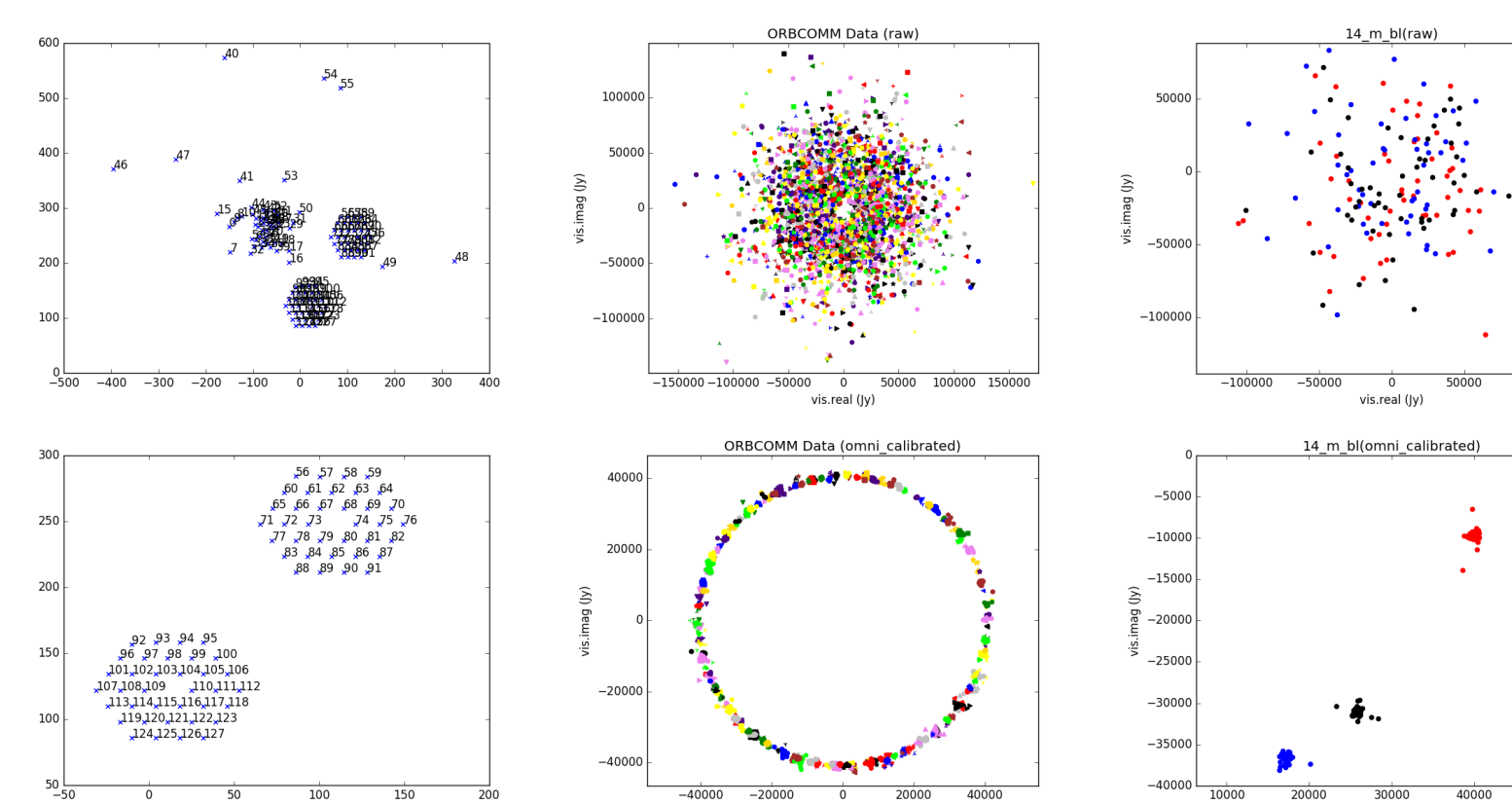


Figure 5: Top left: MWA PhaseII configuration. Middle top: raw ORBComm complex visibility data at 137.1MHz. Each combination of color and shape stands for data from a unique type of baseline. Middle bottom: ORBComm data after redundant calibration. Right top: raw 14m baseline data. Right bottom: calibrated 14m baseline data.

Simulation

The particular characteristics of an array can introduce unexpected effects into the data. To detect a signal as weak as the EoR, understanding and mitigating instrumental effects is critical. For this reason, much effort has been put into simulating the full analysis pipeline, from the point and diffuse sources on the sky to the raw visibilities that come out to the power spectrum estimations.

Fast Holographic Deconvolution (FHD) is a purpose-built software framework for analyzing MWA data. FHD does foreground subtraction by *forward modeling*, which builds a simulated data set, including instrumental effects, and subtracts it from the actual data. This forward modeling feature can also be used as a standalone simulation tool, to generate raw visibilities of foregrounds, noise, and EoR off of existing and future 21cm experiments.

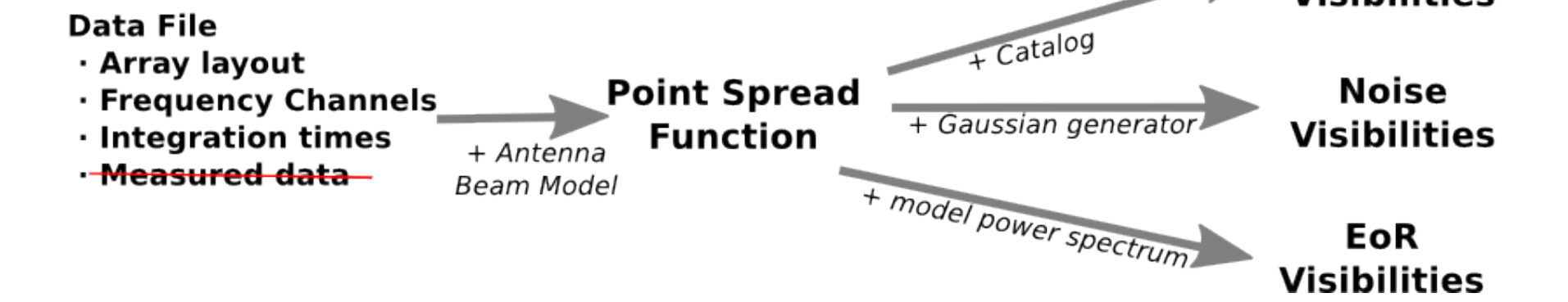


Figure 6: A sample data file (or generated data file) holds array coordinates over time and the frequency channels of the instrument. Given a beam model for the antenna, FHD calculates the full synthesized beam (or point-spread function) for a particular time and set of frequencies. The synthesized beam can then convert a sky catalog into a set of foreground visibilities for the instrument. External EoR simulations can also be fed in to test EoR sensitivity, or Gaussian noise can be injected to simulate noise.

Radio Telescope Arrays



Figure 7: Precision Array for Probing the Epoch of Reionization (PAPER) - Located in South Africa in the Karoo desert, consists of 128 dipole antennas and is considered a 1st generation radio telescope array. PAPER is a redundant array configuration, which means it redundantly probes many of the same k_{\perp} modes and allows for the use of redundant calibration.



Figure 8: Murchison Widefield Array (MWA) - Located in Western Australia in the Murchison Radio Astronomy Observatory. The MWA is a multipurpose array that is used for additional observations such as ionosphere studies and transient radio signals. It consists of 128 tiles which are each made up of 16 dipole antennae. The MWA array configuration is maximized for uv coverage which improves the imaging capability of the array. MWA is a pathfinder project for the Square Kilometer Array (SKA).



Figure 9: Hydrogen Epoch of Reionization Array (HERA) - Located at the same site as PAPER in the Karoo desert. The current phase of HERA consists of 19 14m parabolic dishes. HERA is also a pathfinder project for the SKA.